

Deep tree-ensembles for multi-output prediction

Felipe Kenji Nakano^{a,b,*}, Konstantinos Pliakos^{a,b}, Celine Vens^{a,b}

^a*KU Leuven, Campus KULAK, Faculty of Medicine, Etienne Sabbelaan 53, 8500 Kortrijk, Belgium*

^b*Itec, imec research group at KU Leuven, Etienne Sabbelaan 53, 8500 Kortrijk, Belgium*

Abstract

Recently, deep neural networks have expanded the state-of-art in various scientific fields and provided solutions to long standing problems across multiple application domains. Nevertheless, they also suffer from weaknesses since their optimal performance depends on massive amounts of training data and the tuning of an extended number of parameters. As a countermeasure, some deep-forest methods have been recently proposed, as efficient and low-scale solutions. Despite that, these approaches simply employ label classification probabilities as induced features and primarily focus on traditional classification and regression tasks, leaving multi-output prediction under-explored. Moreover, recent work has demonstrated that tree-embeddings are highly representative, especially in structured output prediction. In this direction, we propose a novel deep tree-ensemble (DTE) model, where every layer enriches the original feature set with a representation learning component based on tree-embeddings. In this paper, we specifically focus on two structured output prediction tasks, namely multi-label classification and multi-target regression. We conducted experiments using multiple benchmark datasets and the obtained results confirm that our method provides superior results to state-of-the-art methods in both tasks.

Keywords: Ensemble Learning, Deep-Forest, Multi-output prediction, Multi-target regression, Multi-label classification

*Corresponding author

Email addresses: felipekenji.nakano@kuleuven.be (Felipe Kenji Nakano), konstantinos.pliakos@kuleuven.be (Konstantinos Pliakos), celine.vens@kuleuven.be (Celine Vens)

1. Introduction

Modern technological advances have opened new horizons in many areas of science. Along with new opportunities and possibilities that were deemed unfeasible in the past, this ongoing progress has given birth to new challenges for the scientific community, stimulating new lines of research [1]. When it comes to the field of machine learning, traditional approaches need to adapt and tackle the new challenges that have emerged (e.g. increased data volume and complexity, need for scalability, etc.) [2].

In this direction, deep learning has arisen as a cutting edge methodology. In recent years, deep learning has expanded the state-of-the-art in diverse fields of knowledge and application domains, such as medicine [3], genomics [4], and self driving cars [5].

Apart from its blatant success, deep neural networks may also present some drawbacks. In most of the scenarios, the training consists of tuning a massive number of parameters which demands considerably large training datasets. This often leads to an extreme computational complexity. In addition, deep neural networks often fail to meet high prediction performance when it comes to small scale datasets, which are still mainstream in many application domains. For instance, studies that follow participants over time (e.g. patients in the context of clinical studies) typically have a limited number (often in the range of a few hundreds) of subjects.

In typical supervised learning, a prediction function is formed on a training set of instances in order to predict a target value [6]. Each instance is represented by a feature vector and associated with a target, which can be categorical (classification) or numerical (regression). Single target prediction tasks adopt the assumption that an instance is associated with a single output variable. However, this assumption does not hold in many real-world problems, as instances may belong to more than one class at the same time. For example, an article can be associated with multiple topics simultaneously. Multi-output prediction

models that learn to predict multiple output variables at the same time are of high importance in this setting. Multi-output prediction, which is also denoted as multi-target prediction [7], is a generalization of multi-target regression and multi-target classification. Multi-label classification can be considered as a special case of multi-target regression (or classification) with only two numerical values (classes) for each target (0 or 1) [8]. Nowadays, due to the increasing volume and complexity of the stored data, multi-output prediction methods draw growing attention. Such approaches boost prediction performance, exploiting the structure of the target space, while being computationally efficient. In this direction, here we focus on multi-output prediction tasks. In particular, we tackle the bottlenecks from deep neural networks by proposing a novel deep tree-ensemble method, where tree-ensembles are built in multiple layers following a deep learning architecture. Our work is motivated by the deep forest approach proposed by Zhou & Feng [9], where the model also consists of several layers. In each layer of [9], a random forest [10] model outputs a class probability vector which is then used to extend the original input feature set. Different from [9], in our approach we include a tree-based representation learning step in every layer extending the original input space with low-dimensional tree-embeddings. More specifically, instead of simply using the predictions of the previous layer as extra attributes for the next one, we learn a high dimensional representation based on the decision paths of the trees in the tree-ensemble collection. Next, we project these high dimensional and sparse vectors to a low-dimensional space, yielding compact tree-embeddings which we use to extend the input feature set.

Our main hypothesis is that adding a representation learning component to the deep forest methodology will boost the predictive performance of the method while keeping the computational complexity low. The nodes of each tree of the ensemble are considered clusters that comprise the instances that are associated to them by the recursive partitioning procedure. The ensemble is converted into a binary vector where each item is associated with a cluster node. If a training instance has passed through this node the corresponding item receives the value of 1, otherwise 0. Tree-ensemble models are trained

over the original feature set in a supervised learning way and therefore the constructed features incorporate label information. It has been shown that such representations benefit from the learning mechanism of tree-ensembles and are apt to boost the performance of subsequently applied prediction models [11]. Furthermore, we filter and apply weights to this binary representation, based on the number of instances that are contained in a cluster (tree node). The decision paths of the individual trees of the ensemble are transformed to high dimensional and label-aware representations. Finally, we transfer these high dimensional feature vectors to a low dimensional space, removing noise and making the resulting compact tree-embeddings computationally efficient. Low-dimensional tree-embeddings were proved highly representative and effective in multi-output prediction tasks [12].

Driven by the great importance and potential of multi-output prediction as well as by the relative lack of deep-forest methods for multi-output tasks, we deploy our proposed deep tree-ensemble (DTE) method to specifically address the tasks of multi-target regression and multi-label classification. Experiments on benchmark datasets from both domains demonstrate that our method is capable of providing superior results with statistical significance when compared to state-of-the-art methods.

The main contributions of this work are summarized below:

- A new state-of-the-art deep tree-ensemble method for multi-target regression and multi-label classification;
- The first study that incorporates representation learning and specifically low-dimensional tree-embeddings into a deep-forest architecture;
- An effective stopping criterion to determine the optimal number of layers as well as mechanisms to surpass overfitting;
- An extensive evaluation on 21 datasets, comparing our approach to state-of-the-art methods;

The remainder of this paper is organized as follows: Section 2 brings a brief overview on multi-target regression, multi-label classification and deep-forest based methods; Section 3 introduces our proposed method; Section 4 presents our experimental setup, and Section 5 contains our results and discussion. Finally, Section 6 contains our final conclusions and future work directions;

2. Related work

In this section, we present a brief overview on relevant literature in multi-label classification and multi-target regression, covering the most popular methods in these fields. For a complete literature survey, we refer the reader to [8, 13, 14].

Despite the great variety of methods, they can be roughly categorized into two approaches: global and local. The global approach corresponds to models that learn to predict all targets at once. Typically, a traditional algorithm, such as decision trees [15], is adapted to handle the constraints of the problem. Different from that, the local approach builds several models which learn to predict different subsets of outputs [16, 17]. In this case, the predictions of all models are combined to provide the final prediction.

2.1. Multi-target regression

Given a set of instances X and a continuous output set $Y \in R^m$, multi-target regression is defined as the task of learning a function f which, for every unseen instance $x \in X$, outputs $y \in Y$, with y being the target set associated with x [13].

Kocev *et al.* [18, 19] proposed global ensembles of predictive clustering trees for structured output tasks. Their experiments showed random forests [10] as the ensemble method that generally yields superior results. Using deep neural networks, Du and Xu [20] proposed a hierarchical neural networks method which employs a divide-and-conquer (local) approach. More specifically, it decomposes the original multi-target problem into several local sub-tasks, and combine their

solutions. Also using deep neural networks, Zhen *et al.* [21] proposed a general model that employs a non-linear layer and a linear low-rank layer to perform direct face alignment via multi-target regression. ERC [22] is an ensemble local approach where multiple regressors are chained in a random order. In this method, a separate regressor is built for each target and its predictions are used as extra attributes for the next regressor. Similarly to ERC, DSTARS [16] also chains multiple stacked regressors. Its main difference consists of using the feature importance to identify target correlations, in the sense that, targets with positive feature importance values are used as extra attributes for the next regressors.

2.2. Multi-label classification

Given a set of instances X and a discrete output set Y , multi-label classification is defined as the task of learning a function f which, for every unseen instance $x \in X$, outputs $y \in Y$, with y being the label set associated with x [13].

Based on lazy learning, ML-KNN [23] is an extended version of the traditional k-nearest neighbours, which in addition to finding the closest instances from the training dataset, also employs the concept of maximum a posteriori to predict the labels of new instances. Proposed by Tsoumakas *et al.* [17], Rakel is a local ensemble method which aims to reduce the size of the label set by separating it into smaller random subsets. Next, one model is built per set and the predictions are combined. As an extension of Rakel, Wang *et al.* [24] proposed to select the subsets of labels based on an active learning algorithm, rather than at random. Their results show that the performance can be improved by selecting the best group of labels per subset. Adopting the notion of missing labels, Ma and Chen [25] proposed a method that imposes low-rank matrix structures in both global and local manner. More precisely, it enforces local low-rank on predictions with the same labels, whereas the rank is expanded for predictions with different labels.

2.3. Deep-Forest based methods

Similarly to the single output deep forest approach [9], its multi-label version proposed in [26] employs multiple layers of random forests and extra trees [27]. However, prediction probabilities are evaluated using measured-based confidence values. More specifically, if the prediction probabilities from the current layer have a better confidence than the ones from the previous layer, they are updated. As an extension of the multi-label deep-forest, Wang *et al.* [28] addressed weak-label learning by using a label complement procedure. At each layer, the label set of the training dataset is complemented using an inner cross-validation scheme, that is, if the label is predicted as positive its label is changed in the training dataset.

Gao *et al.* [29] proposed a deep-forest variant that includes the oversampling method SMOTE [30] to address imbalanced tasks. All instances that belong to the minority class and were misclassified in the previous layer are used as input to SMOTE, the new generated instances are concatenated with the dataset and a new layer is built.

In the oncology field, Su *et al.* [31] proposed a deep forest model to predict anti-cancer drug response. The original deep forest was extended by allowing the usage of two feature sets and including a feature optimization method after each layer. Ma *et al.* [32] proposed a cost-sensitive version for price prediction. First, the prices are discretized using K-means, next the authors employed a deep-forest method which penalizes wrong predictions according to how inaccurate they are. In the context of hashing for image retrieval, Zhou *et al.* [33] demonstrated that the original deep-forest is capable of learning a hashing function that outperforms deep learning hashing methods.

3. The proposed method

In this section, we thoroughly present our deep tree-ensemble (DTE) method. At first, we introduce the general framework, focusing on its main components. Next, we present a detailed description of the proposed representation learning

components. Finally, we introduce the stopping criterion that was employed as well as specific characteristics of our architecture.

3.1. The general framework

Inspired by recent advances on deep-forest models, our proposed method also employs a cascade of layers of tree ensembles. The main difference relies on the introduced representation learning component at each layer. More specifically, our proposed model extends the original framework by including low-dimensional tree-embeddings, a promising representation learning method, which is further explained in the next subsection.

It is widely known that diversity among the underlying models is a crucial component in any ensemble method [34]. Hence, each layer of our model consists of a set of different tree-ensemble models. Let $B = \{\beta_1, \dots, \beta_i, \dots, \beta_{|B|}\}$ be the different models. Each β_i corresponds to a tree-ensemble model such as random forest (RF) [10], extremely randomized trees also known as extra-trees (ET) [27], gradient boosting, etc. The number $|B|$ also varies across different applications. Here, we build our deep tree-ensemble (DTE) method using one RF and one ET model ($|B| = 2$) per layer. We employ these two models as they are well established and also powerful. Moreover, we follow the setting of predictive clustering trees [15] due to its natural clustering and variance reduction characteristics.

Our proposed framework is illustrated in Figure 1. Initially, the original feature representation (X) is used as input. RF and ET are employed to create their respective tree-embeddings F . Let F_{RF} and F_{ET} be the RF and ET based tree-embeddings, respectively.

Next, the original feature representation (X) is concatenated with the generated representations (F), and crossed over to be used as input for the models that perform predictions. That is, the F_{RF} is generated in the current layer and given as input to ET, and vice-versa. Our main motivation behind this is that each β_i benefits from learning from representations that were yielded by β_j , where $i \neq j$. This way, we increase the diversity between the predictors. Each

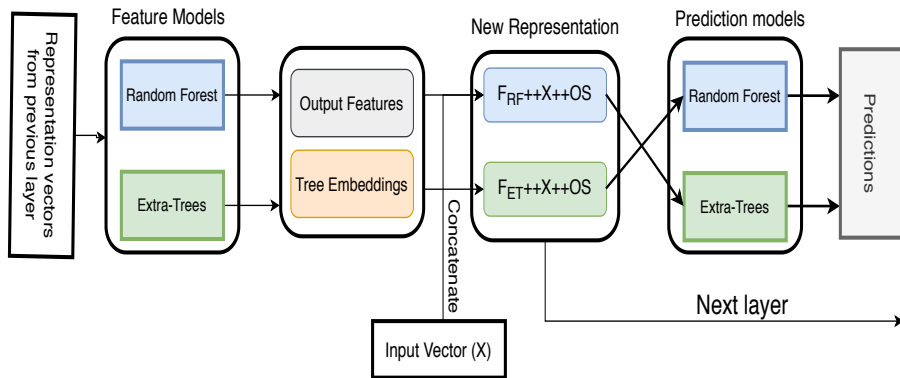


Figure 1: An example of a layer of our proposed model.

model β_i is always built using representations that stem from different models. Besides boosting diversity, we assume that this step contributes to avoid overfitting.

Thus, for all layers L with $L \geq 1$, a RF model is trained using $X \# F_{ET}$ features, and an ET model with $X \# F_{RF}$, where $\#$ corresponds to vector concatenation. This can be generalized to $|B|$ tree-ensemble models; $\forall \beta_i \in B$ the generated feature set is $X \# F_{\beta_1} \# F_{\beta_j} \# \dots \# F_{\beta_{|B|}}$, where $j \neq i$. These models are chained to the DTE, building a new layer. This procedure is repeated until the stopping criterion is triggered.

When it comes to final predictions, our method employs all the models $\beta_i \in B$ of its last layer (w.r.t the stopping criterion). More specifically, it averages the output of all trees in all tree-ensemble models β_i to perform predictions.

It is possible to implement different feature representation combinations. For instance, output features as used in [9, 26] could be included in our architecture, allowing us to propose four variants of our method:

- X.TE: Original feature representation and tree-embeddings ($X \# F$);
- X.OS: Original features and prediction (i.e., output space) features. This variant is identical to the original deep-forest [9], except for the feature cross-over.

- X_OS_TE: Original features, tree-embeddings and prediction features;
- TE: Only tree-embeddings. A baseline variant which is used to evaluate the importance of concatenating the original feature representation with the generated one.

3.2. Low Dimensional Tree-embeddings

Originally proposed for biomedical data, tree-embeddings provide more informative and variant representations by exploiting the inner properties of decision trees, in particular, the clustering performed at each split is converted to a new feature representation [12].

Given a trained ensemble of decision trees, tree-embeddings are generated using the following procedure. Initially, all the trees are converted to a binary vector where each position is associated with a node. These vectors are concatenated, resulting in $C = \{c_1, c_2, \dots, c_{|C|}\}$, $|C|$ being the total number of nodes in the ensemble. By treating $c \in C$ as a feature, we create a new representation $F \in R^{N \times |C|}$ where N stands for the number of instances in the dataset. The values in F are instantiated according to how instances traverse the trees. Namely, F_{ij} equals to 1 if such instance i belongs to node (cluster) j , otherwise its value is set to 0, as exemplified in Figure 2. In more detail, in 2, we show a hypothetical instance being classified into leaf nodes 4 and 10. Next, we show the binary vector representation for the instance, where colored circles correspond to vector positions set to 1.

Secondly, we discard the nodes in F (columns $F_{\cdot j}$) which are present in more than $p\%$ of the instances, removing non-meaningful nodes, such as the ones located close to the root and the root itself. Next, the remaining nodes are weighted according to Equation 1 where nodes that contain many instances are credited a lower weight, and the opposite is valid for more representative nodes. In Equation 1, w_j stands for the weight assigned to node j , $|c_j|$ is the number of

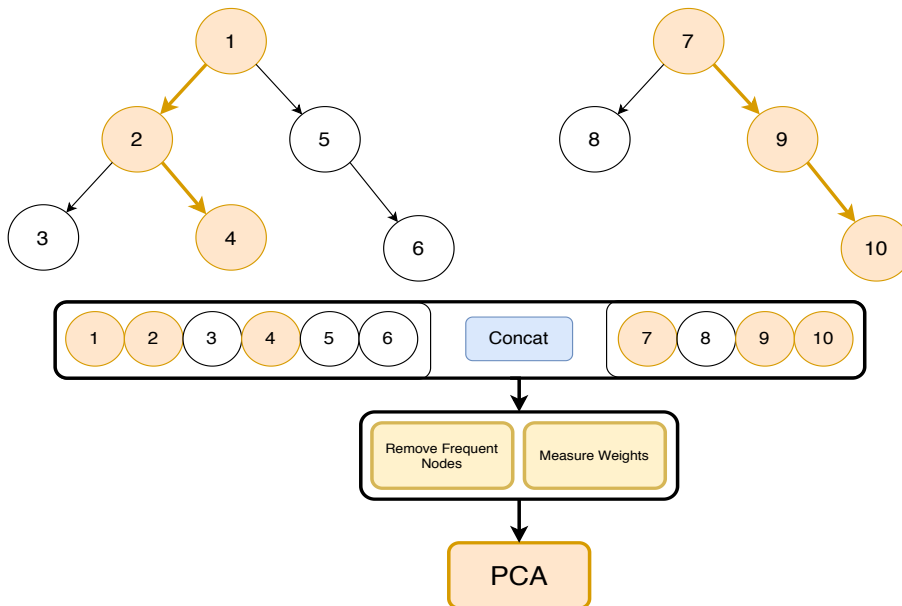


Figure 2: Hypothetical example being classified by leaf nodes 4 and 10.

instances that transverse j and e is a small positive value for numerical stability.

$$w_j = \frac{1}{\log(|c_j|) + e} \quad (1)$$

Lastly, the filtered and weighted vectors are transferred from their high dimensional space to a lower dimensional one. Pliakos and Vens [12] evaluated several standard methods in this context, such as: PCA, kernel PCA, independent component analysis and truncated singular value decomposition. The results obtained from their experiments have showed that PCA is often associated with superior results. Hence, here we also employ PCA to obtain the final tree-embeddings.

This way, through this representation learning component, we yield a compact but yet informative and target-aware representation. By transferring the tree-path features to a low dimensional space we make our approach computationally more efficient removing as well any existing noise. Moreover, by tuning the number of kept components (final dimensionality of the F space) we implic-

itly assign a latent weight to the added feature set, in relation to the original space X . Thus, we can control the number of added features. Recall that, this procedure is performed separately for each ensemble model (β_i) due to the embeddings cross-over mechanism, as shown in Figure 1.

Furthermore, considering that tree-embeddings are very representative and label-aware, overfitting can be an issue. Thus, we employ the following procedure:

Overfitting prevention: The ensembles in the model itself are not used to generate tree-embedding features. A separate RF and an ET are built using a random sample of the training dataset, these models are used exclusively for the generation of tree-embeddings, and, thus, are not used to perform predictions..

3.3. Output space features

Recently, features based on the output of models have been vastly exploited in structured output prediction [26, 16, 35]. More precisely, given a chain of models, the outputs (i.e., predictions) of the previous models are used as extra (induced) features for the next one.

These features are known to enrich the representational power by exploiting label correlations among the output set [16]. Furthermore, it also allows the models to learn from each other’s mistakes [36], enhancing the overall performance. Likewise, output features are commonly exploited in deep-forest models [9, 26].

Thus, we also incorporate them into our model. Moreover, analogously to tree-embeddings, we also employ an overfitting prevention measure to obtain output features.

Overfitting prevention: The ensembles in the model itself are not used to generate output features. Similarly to [9, 26], an inner K -fold cross validation is employed, resulting in $2K$ separate models (RF + ET). Their averaged outputs, either prediction probabilities or target values, are the output features.

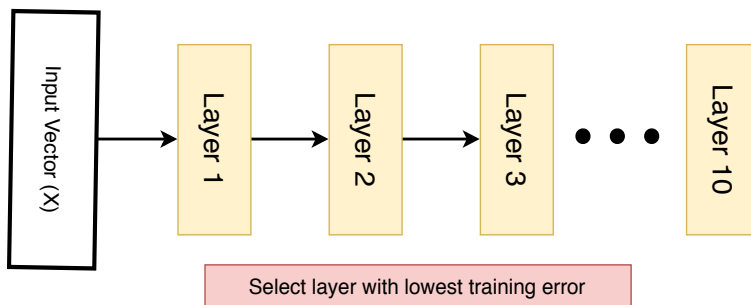


Figure 3: Proposed stopping criterion. Select the layer with the lowest training error given a pre-defined number of layers

Using hard predictions (0 or 1) as extra attributes, especially for multi-label classification, could also be implemented, as proposed by Read [35]. Nonetheless, there has been an increasing tendency to use the raw output of the models due to superior results [37].

3.4. Stopping criterion

As for the stopping criteria, different options can be explored. At a first glance, the training could be stopped immediately after any deterioration in the performance. It is also possible to establish a tolerance level. For instance, the training can be interrupted if the performance does not improve after a certain number of layers as proposed by [26]. Both measures may lead to sub-optimal solutions due to premature stops. As a countermeasure, we propose a new stopping criterion.

Given a pre-defined number of iterations, we select the layer with the best performance on the training dataset. Thus, all the ensembles trained after the layer with the best performance are discarded. The final model consists of all tree-ensembles up to the layer with the best performance, and the output of this layer yields the final predictions. This stopping criterion is exemplified in Figure 3.

4. Experimental Setup

4.1. Multi-target regression

In Table 1, we present the multi-target regression datasets used in this work.

4.1.1. Datasets

Datasets	#Instances	#Features	#Targets	#Domain
atp1d	337	370	6	Air ticket price over a day
atp7d	296	370	6	Air ticket price over 7 days
oes97	334	263	16	Number of employees per job measured in 1997
oes10	403	298	16	Number of employees per job measured in 2010
edm	154	16	2	Electrical discharge of machinery
sf1	323	10	3	Occurrence of solar flares over a period of 24h
sf2	1066	9	3	Occurrence of solar flares over a period of 24h(v2)
jura	359	15	3	Heavy metal concentration
wq	1060	16	14	Fauna and flora in Slovenian rivers
enb	768	8	2	Heating and cooling of efficient buildings
slump	103	7	3	Concrete quality
andro	49	30	6	Water quality
osales	639	401	12	Online sales of a product over its first month
scpf	1137	23	3	Number of views, clicks and comments

Table 1: Multi-target regression datasets characteristics

We have collected a total of 14 benchmark datasets from a public repository¹ and split them using 10 fold cross-validation. The resulting folds are available at². In terms of characteristics, they range from a very small number of features and targets (Slump) to 401 features (Osales) and 16 targets (oes97 and oes10).

4.1.2. Comparison methods

- DSTARS: A recently proposed approach which combines multiple stacked models into a deep structure [16], available at³. The results associated to DSTARS were imported directly from the original manuscript since we are using the same data partitions;
- MLP: A comparative multi-layer perceptron neural network regressor⁴;

¹<http://mulan.sourceforge.net/datasets-mtr.html>

²The link will be provided upon acceptance.

³<https://github.com/smastelini/mtr-toolkit>

⁴<https://scikit-learn.org/stable/>

- RF + ET: A shallow version of our proposed method which consists of a single layer with one RF and one ET; ⁵;
- Our proposed method: We compare all the four variants of our method: TE, X_TE, X_OS, X_TE_OS ⁶;

For RF + ET, we have optimized (inner 5 fold cross-validation tuning) the number of trees considering these values {10, 20, 50, 100, 150, 200}.

For the MLP, we have also employed an inner 5-fold cross validation to optimize the number of layers and neurons. More specifically, we have considered the following values: number of neurons {50,100} and number of layers {1,2}. The activation function and solver were fixed to ReLu and ADAM, respectively.

For the number of PCA components in our method, we have optimized the number of components considering a percentage of the total number of decision path features {1 component, 1% , 5%, 20%, 40%, 60%, 80%, 95%} multiplied by $\min(N, |c|)$, N being the number of instances in the dataset and $|c|$ the number of nodes in the ensemble. The number of trees is also optimized considering the same values {10, 20, 50, 100, 150, 200} and output features are generated using 5-fold cross validation. As for preventing the overfitting which may be associated with tree-embeddings, we have employed random samples which contain 50% of the training dataset. Finally, we run our model with a maximum of 10 layers.

4.1.3. Evaluation Measures

Similar to related literature, we are employing the aRRMSE (Average Relative Root Mean Squared Error). RRMSE is the square root of the mean squared error (RMSE) of the model divided by the RMSE of a default model that predicts the average target value in the training set. Likewise, aRRMSE is computed by taking the average RRMSE of all targets. Formally, Equation 2 presents aRRMSE where \hat{y} stands for predicted values, \bar{y} represents the average

⁵<https://scikit-learn.org/stable/>

⁶The link will be available upon acceptance

value, M is total the number of targets and N is the number of testing instances.

$$aRRMSE = \frac{1}{M} \sum_{t=1}^M \sqrt{\frac{\sum_{i=1}^N (y_t^i - \hat{y}_t^i)^2}{\sum_{i=1}^N (y_t^i - \bar{y}_t^i)^2}} \quad (2)$$

4.2. Multi-label classification

In this section, we provide details on the multi-label experimental setup.

4.2.1. Datasets

In Table 2, we present statistical information about the dataset used.

Datasets	#Instances	#Features	#Labels	# Cardinality	#Application
birds	645	260	19	1.01	Species recognition based on chirping
CAL500	502	68	174	26.04	Instrument, genre and voice identification
emotions	593	72	6	1.87	Emotion recognition from songs
enron	1702	1001	53	3.38	Email classification
medical	978	1449	45	1.25	Diagnosis based on clinical text
scene	2407	294	6	1.07	Image annotation
yeast	2417	103	14	4.24	Protein function prediction

Table 2: Multi-label classification datasets characteristics

As can be seen, the datasets belong to different domains of applications, including sound recognition (Birds, Emotions and CAL500), image annotation (Scene), email classification (Enron) and medical and biomedical applications such as Medical and Yeast.

There is also a wide variation in the number of features and labels. Certain datasets present fewer features such as CAL500 and Emotions with 68 and 72, respectively, whereas Medical presents 1449 features. The number of labels also varies significantly, ranging from 6 up to 174.

We have collected them from a public repository⁷, concatenated the train and test subsets, and performed 10 fold cross-validation. The resulting folds are available at ⁸.

⁷<http://mulan.sourceforge.net/datasets-mlc.html>

⁸The link will provided upon acceptance.

4.2.2. Comparison methods

We have compared the following multi-label methods:

- Raket: An ensemble approach which builds a base classifier per subset of labels [17] ⁹.
- MLKNN: A multi-label version of the baseline K-Nearest-Neighbours classifier [23] ¹⁰;
- MLDF: A recently proposed multi-label deep-forest version proposed in [26], available at ¹¹;
- MLP: A comparative multi-layer perceptron neural network multi-label classifier ¹²;
- RF + ET: A shallow version of our proposed method which consists of a single layer with one RF and one ET; ¹³;
- Our proposed method: We compare all the four variants of our method: TE, X_TE, X_OS, X_OS_TE ¹⁴;

For Raket, we have employed SVMs with linear kernel as base classifiers and random subsets of size 3. For MLKNN, we have optimized K considering the values {3,5,7} and S {0.5, 0.7, 1.0} using a 5-fold inner cross validation.

For our main competitor, MLDF, we have employed the same parameters from their original manuscript. That is, 1 random forest and 1 extra tree, 40 trees at the first layer, increasing 20 trees per layer up to 100, 5-fold inner cross-validation to generate the output features. As the stopping criteria, the training is interrupted after the addition of 3 layers without improvement. Since this

⁹<http://scikit.ml/>

¹⁰<http://scikit.ml/>

¹¹http://www.lamda.nju.edu.cn/code_MLDF.ashx

¹²<https://scikit-learn.org/stable/>

¹³<https://scikit-learn.org/stable/>

¹⁴The link will be available upon acceptance

Y	True label set
X	Instance set
Z	Predicted labels
TP	True positive
FP	False positive
FN	False negative
S	Size of set S
N	Number of instances ($ X $)
M	Number of labels in Y ($ Y $)
θ	Ranking function
I	Indicator function, returns 1 if its argument evaluates to True
\hat{Y}_i	Complement of Y for an instance i
\oplus	Boolean XOR

Table 3: Table with symbols used to describe the multi-label evaluation measures.

method is measure dependent, we have compared it using the measures with which it is defined.

The parameters related to the MLP, RF + ET and the variants of our proposed method were optimized in the same manner as in the multi-target regression experiments.

4.2.3. Evaluation Measures

In Table 3, we present the symbols used to describe our multi-label evaluation measures.

The hamming loss (Equation 3) measures the average number of labels wrongly predicted. In this case, we have applied a threshold of 0.5 to obtain Z .

$$HammingLoss = \sum_i^N Z_i \oplus Y_i \quad (3)$$

Based on the ranking of the predicted labels, one error, Equation 4, measures the average number of times that the label with highest prediction probability

(lowest rank) is not a true label.

$$OneError = \frac{1}{N} \sum_i^N I(\operatorname{argmin}_{y \in Y} \theta(y) \notin Y_i) \quad (4)$$

Also based on ranking, the ranking error (Equation 5) measures the average proportion of labels that were ranked incorrectly.

$$RankingError = \frac{1}{N} \frac{1}{|Y_i| |\hat{Y}_i|} |(y_1, y_2) : \theta_i(y_1) > \theta_i(y_2), (y_1, y_2) \in Y_i \times \hat{Y}_i| \quad (5)$$

We are also employing the mean average precision. Due to possible imbalance in the label set, we are employing its micro variant described at Equation 6.

$$MicroAveragePrecision = \sum_i^N \sum_j^M \frac{TP_{ij}}{TP_{ij} + FP_{ij}} \quad (6)$$

The MicroAUC is obtained by measuring the area under the curve generated by using the recall (Equation 7) in the x-axis and the false positive rate (FPR, Equation 8) in the y-axis.

$$Recall = \frac{TP}{TP + FN} \quad (7)$$

$$FPR = \frac{FP}{FP + TP} \quad (8)$$

5. Results and Discussion

Initially, we present the results on multi-target regression, followed by multi-label classification. More results concerning other stopping criteria are available in the Appendix.

5.1. Multi-target regression

As can be seen in Table 4, our proposed method provides the best results in the majority of the cases. More specifically, the variant X_OS_TE outperforms the other methods. When compared to the literature method,

Datasets	RF+ET	MLP	X_TE	TE	X_OS	X_OS_TE	DSTARS
atp1d	0.386	0.456	0.379 ^{5.5}	0.398 ^{1.4}	0.377 ^{7.1}	0.369 ^{6.0}	0.390 ^{2.9}
atp7d	0.504	0.567	0.506 ^{4.6}	0.533 ^{1.5}	0.49 ^{6.4}	0.494 ^{5.5}	0.514 ^{3.0}
oes97	0.552	0.661	0.549 ^{5.4}	0.583 ^{3.0}	0.546 ^{4.6}	0.552 ^{4.6}	0.514 ^{2.5}
oes10	0.424	0.611	0.416 ^{5.2}	0.45 ^{1.9}	0.425 ^{4.9}	0.42 ^{6.3}	0.407 ^{2.6}
edm	0.55	0.917	0.522 ^{7.2}	0.57 ^{4.7}	0.487 ^{7.1}	0.482 ^{8.4}	0.676 ^{2.2}
sf1	0.737	0.983	0.698 ^{5.9}	0.764 ^{1.7}	0.746 ^{5.9}	0.739 ^{6.8}	1.00 ^{1.1}
sf2	1.159	1.852	0.92 ^{3.1}	0.948 ^{1.6}	1.155 ^{6.5}	0.821 ^{4.6}	0.857 ^{1.6}
jura	0.48	0.698	0.459 ^{6.0}	0.564 ^{3.4}	0.421 ^{6.0}	0.42 ^{6.2}	0.590 ^{3.3}
wq	0.624	0.202	0.627 ^{5.7}	0.624 ^{1.0}	0.618 ^{7.4}	0.627 ^{5.1}	0.910 ^{1.1}
enb	0.132	0.244	0.104 ^{6.9}	0.109 ^{2.0}	0.101 ^{6.8}	0.106 ^{5.0}	0.114 ^{2.6}
slump	0.436	0.347	0.424 ^{4.1}	0.504 ^{2.5}	0.393 ^{4.1}	0.388 ^{5.2}	0.833 ^{3.0}
andro	0.515	0.434	0.508 ^{4.1}	0.694 ^{3.0}	0.496 ^{3.2}	0.5 ^{6.5}	0.658 ^{4.0}
osales	0.577	0.873	0.566 ^{6.2}	0.63 ^{3.2}	0.555 ^{3.7}	0.542 ^{6.6}	0.728 ^{4.3}
scpf	0.653	1.024	0.588 ^{5.8}	0.711 ^{4.4}	0.595 ^{6.0}	0.576 ^{4.9}	0.901 ^{2.1}
mean	0.552	0.705	0.519 ^{5.41}	0.577 ^{2.52}	0.529 ^{5.69}	0.503 ^{5.84}	0.649 ^{2.53}

Table 4: Performance in terms of aRRMSE for multi-target regression. The numbers above the measures correspond to the mean number of layers in the final model.

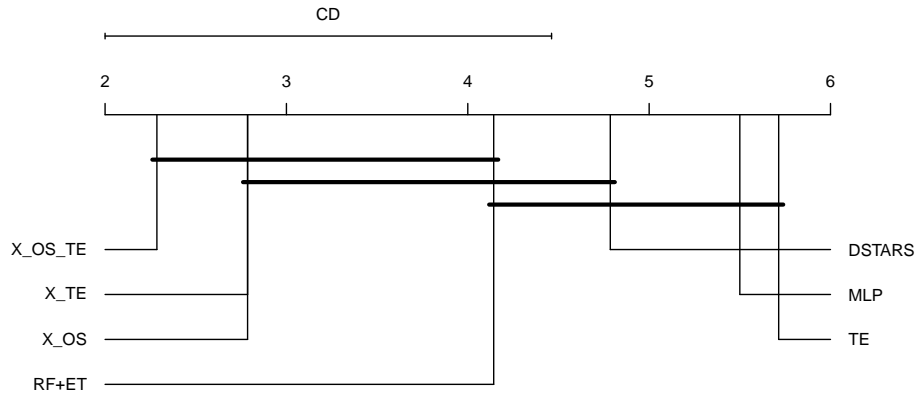


Figure 4: Friedman-Nemenyi comparing the multi-target regression methods.

DSTARS, X_OS_TE managed to be statistically significantly better according to the Friedman-Nemenyi test (Figure 4).

The second best method, on average, is the X_TE variant with a slight margin over the third best method, X_OS. This finding demonstrates that both types of features are capable of enriching the original feature set, nonetheless they should be combined to achieve optimal performance.

Opposed to that, the TE variant provided underwhelming results in most cases. It also limited itself to shallower models due to its performance sequentially decreasing on the training dataset. This as a clear indication that tree-embeddings should be used to augment the original features and not entirely replace them. Hence, it highlights the necessity of using the original features (X) with the extra features since all variants of our method manage to be superior than the baseline RF + ET, except TE itself.

These results also validate our stopping criterion. In comparison to the results obtained with different stopping criteria, our performance is superior to immediately stopping the training after deterioration (Appendix Table 1), and it approaches the best performance in the test (Appendix Table 2).

In addition, despite having a maximum of 10 layers, the average number of layers of the best variant, X_OS_TE, is approximately 6, whereas DSTARS converges on average with 2.5 layers. Since DSTARS relies mostly on output features, this can indicate that tree-embeddings allow the model to grow deeper and consequently learn more complex patterns.

DSTARS provided the best performance in two cases, oes97 and oes10. However, it underperformed in the other datasets, leading to a worse average result. Similarly, the MLP managed to provide the best results in some cases, nonetheless its average performance was worse.

5.2. Multi-label classification

Datasets	RF+ET	Rakel	ML-KNN	MLP	MLDF	X_TE	TE	X_OS	X_OS_TE
Label Ranking Error ↓									
birds	0.014	0.468	0.537	0.482	0.329 ^{4.6}	0.012 ^{5.22}	0.038 ^{1.0}	0.013 ^{5.22}	0.013 ^{5.67}

CAL500	0.081	0.49	0.517	0.323	0.643 ^{1.5}	0.081 ^{5.0}	0.1 ^{1.56}	0.083 ^{1.11}	0.083 ^{1.0}
emotions	0.006	0.501	0.497	0.248	0.405 ^{4.6}	0.002 ^{1.11}	0.005 ^{1.0}	0.002 ^{1.56}	0.002 ^{1.11}
enron	0.028	0.415	0.455	0.144	0.311 ^{5.9}	0.029 ^{6.33}	0.046 ^{2.67}	0.028 ^{7.33}	0.03 ^{6.33}
medical	0.022	0.165	1.0	0.147	0.185 ^{11.1}	0.019 ^{6.0}	0.026 ^{1.33}	0.02 ^{7.11}	0.018 ^{7.33}
scene	0.005	0.076	0.13	0.012	0.475 ^{12.2}	0.003 ^{1.33}	0.008 ^{1.22}	0.002 ^{1.0}	0.002 ^{1.0}
yeast	0.001	0.011	0.015	0.003	0.462 ^{7.5}	0.001 ^{3.67}	0.002 ^{1.0}	0.001 ^{1.56}	0.001 ^{1.0}
mean	0.022	0.304	0.45	0.194	0.401 ^{6.77}	0.021 ^{4.09}	0.032 ^{1.4}	0.021 ^{3.56}	0.021 ^{3.35}
One Error ↓									
birds	0.447	0.527	0.537	0.554	0.549 ^{7.0}	0.384 ^{6.67}	0.471 ^{6.11}	0.342 ^{5.11}	0.318 ^{6.44}
CAL500	1.0	1.0	1.0	1.0	1.0 ^{1.0}	1.0 ^{1.0}	1.0 ^{1.0}	1.0 ^{1.0}	1.0 ^{1.0}
emotions	0.142	0.749	0.757	0.377	0.727 ^{3.7}	0.101 ^{5.22}	0.148 ^{4.0}	0.116 ^{5.67}	0.105 ^{7.33}
enron	0.741	0.828	0.832	0.416	0.916 ^{11.3}	0.597 ^{6.44}	0.637 ^{2.78}	0.602 ^{7.67}	0.558 ^{6.22}
medical	0.581	0.27	1.0	0.194	0.45 ^{15.0}	0.34 ^{6.67}	0.36 ^{6.0}	0.413 ^{5.22}	0.357 ^{7.78}
scene	0.194	0.13	0.161	0.021	0.491 ^{9.0}	0.073 ^{4.56}	0.104 ^{7.11}	0.054 ^{6.44}	0.045 ^{7.0}
yeast	0.108	0.059	0.08	0.015	0.831 ^{7.1}	0.058 ^{7.11}	0.095 ^{1.0}	0.071 ^{5.0}	0.056 ^{5.78}
mean	0.459	0.509	0.624	0.368	0.709 ^{7.73}	0.365 ^{5.38}	0.402 ^{4.0}	0.371 ^{5.16}	0.348 ^{5.94}
Hamming Loss ↓									
birds	0.036	0.063	0.053	0.073	0.044 ^{6.9}	0.029 ^{6.44}	0.042 ^{5.33}	0.026 ^{5.44}	0.022 ^{5.67}
CAL500	0.088	0.107	0.086	0.065	0.227 ^{1.1}	0.088 ^{4.33}	0.096 ^{1.22}	0.091 ^{1.11}	0.091 ^{1.0}
emotions	0.027	0.248	0.239	0.112	0.198 ^{4.4}	0.018 ^{5.22}	0.027 ^{3.11}	0.02 ^{5.67}	0.018 ^{7.33}
enron	0.028	0.043	0.034	0.013	0.063 ^{2.1}	0.021 ^{6.89}	0.023 ^{3.0}	0.02 ^{6.44}	0.018 ^{6.78}
medical	0.015	0.008	0.028	0.005	0.014 ^{10.7}	0.009 ^{6.67}	0.009 ^{6.0}	0.01 ^{5.89}	0.009 ^{7.56}
scene	0.034	0.028	0.028	0.004	0.114 ^{7.3}	0.013 ^{4.56}	0.019 ^{6.56}	0.009 ^{6.44}	0.008 ^{6.78}
yeast	0.01	0.005	0.006	0.001	0.204 ^{7.0}	0.006 ^{7.0}	0.01 ^{1.0}	0.006 ^{3.89}	0.005 ^{5.33}
mean	0.034	0.072	0.068	0.039	0.123 ^{5.64}	0.026 ^{5.87}	0.032 ^{3.75}	0.026 ^{4.98}	0.024 ^{5.78}
Micro Average Precision ↑									
birds	0.911	0.092	0.053	0.073	-	0.919 ^{5.11}	0.537 ^{7.33}	0.903 ^{5.22}	0.909 ^{6.44}
CAL500	0.768	0.438	0.514	0.634	-	0.761 ^{5.78}	0.685 ^{7.67}	0.728 ^{6.67}	0.724 ^{8.22}
emotions	0.986	0.472	0.485	0.772	-	0.991 ^{1.0}	0.98 ^{8.22}	0.992 ^{1.0}	0.991 ^{1.0}
enron	0.878	0.428	0.502	0.806	-	0.892 ^{1.0}	0.827 ^{8.22}	0.899 ^{1.0}	0.901 ^{1.0}
medical	0.898	0.741	0.028	0.823	-	0.931 ^{4.78}	0.872 ^{7.11}	0.888 ^{2.0}	0.921 ^{1.0}
scene	0.992	0.864	0.865	0.982	-	0.996 ^{2.56}	0.973 ^{7.78}	0.997 ^{1.0}	0.997 ^{1.0}
yeast	0.998	0.987	0.986	0.997	-	0.999 ^{4.11}	0.994 ^{8.89}	0.999 ^{6.56}	0.999 ^{6.56}
mean	0.919	0.575	0.49	0.727	-	0.927 ^{3.48}	0.838 ^{7.89}	0.915 ^{3.35}	0.92 ^{3.6}
Micro AUC ↑									
birds	0.986	0.56	0.5	0.547	-	0.983 ^{5.11}	0.829 ^{7.56}	0.982 ^{5.22}	0.981 ^{6.0}
CAL500	0.921	0.747	0.74	0.839	-	0.919 ^{6.0}	0.893 ^{7.67}	0.913 ^{6.78}	0.912 ^{8.22}
emotions	0.994	0.696	0.701	0.859	-	0.996 ^{1.0}	0.991 ^{7.89}	0.996 ^{1.0}	0.996 ^{1.0}
enron	0.971	0.775	0.756	0.911	-	0.97 ^{1.0}	0.949 ^{8.22}	0.972 ^{1.0}	0.972 ^{1.0}
medical	0.977	0.904	0.5	0.915	-	0.98 ^{4.78}	0.972 ^{7.11}	0.979 ^{3.89}	0.981 ^{1.0}
scene	0.998	0.951	0.926	0.992	-	0.999 ^{2.56}	0.988 ^{7.78}	0.999 ^{1.0}	0.999 ^{1.0}
yeast	0.998	0.993	0.99	0.998	-	0.999 ^{4.11}	0.996 ^{8.89}	0.999 ^{6.56}	0.999 ^{5.89}
mean	0.978	0.804	0.73	0.866	-	0.978 ^{3.51}	0.945 ^{7.87}	0.977 ^{3.64}	0.977 ^{3.44}

Table 5: Results multi-label classification. The numbers above the measures correspond to the mean number of layers in the final model.

As detailed in Table 5, two variants of our proposed method, X-TE and X_OS-TE, provided the best average results in all evaluation measures.

According to one error and hamming loss, X_OS-TE yields superior results

overall, whereas X_TE has the upper hand in micro average precision and micro AUC. In terms of label ranking error, X_TE, X_OS and X_OS_TE had a similar number of superior performances, nonetheless, on average, they are equivalent.

When analyzing one error and hamming loss, the neural network, MLP, was superior in four datasets (enron, medical, scene and yeast) which contain more instances as seen in Table 2, nonetheless our variants X_TE, X_OS and X_OS_TE were still superior on average. Moreover, when considering micro average precision and micro AUC, the MLP failed to achieve comparable results.

Our main competitor, MLDF, struggled to achieve a competitive performance. With the exception of a few cases, its performance was underwhelming even when compared to the baselines for all three available evaluation measures¹⁵. This finding is rather surprising at first since it is somewhat similar to our variant X_OS. However, there are some major differences between the two methods. First, there is a different optimization mechanism for the number of trees. Second, the extra features used at each layer are different, since X_OS directly concatenates the output features, and MLDF employs a measure-aware feature reuse mechanism. Third, our method also employs cross-over between the extra feature sets to prevent overfitting. The difference is highlighted in Figure 5 where MLDF is associated with a low rank, making it statistically significantly different from our X_TE, X_OS, X_OS_TE variants.

Moreover, similarly to the multi-target regression experiments, the TE variant struggles to perform competitively, instigating the necessity of incorporating the original features. Likewise, the stopping criterion adopted by our method approximates the best possible performance (Appendix Table 4).

It is also noticeable that the number of layers differs from measure to measure. For one error and hamming loss, the optimal averages are roughly 6, whereas label ranking error and the micro measures require 3 and 5, respectively.

¹⁵The extra features employed by MLDF are measure specific, and they are not defined for Micro Average Precision and Micro AUC.

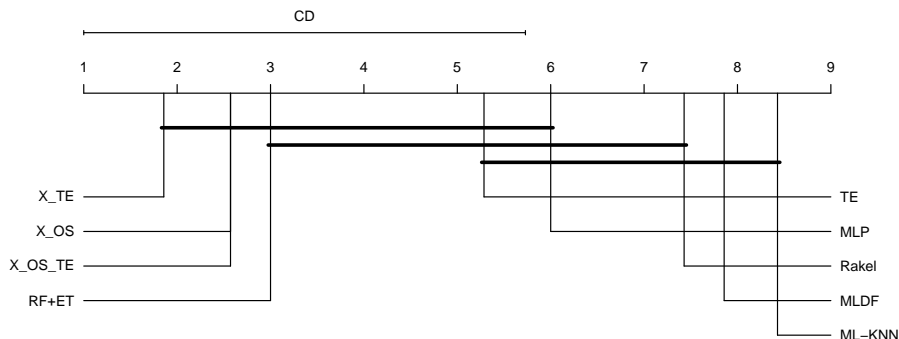


Figure 5: Friedman-Nemenyi test considering the Label Ranking error.

When analyzing the CAL500 dataset, we have noticed that the X_TE variant is constantly superior than the variants X_OS and X_OS_TE in all evaluation measures. We believe that this is related to the number of labels in its label set. Since CAL500 has a relatively large label set, its output features are often similar to sparse vectors, meaning that, in this case, they may hinder the models performance. This is further exemplified by the performance provided by the baseline (RF + ET) which is always superior to all variants with output features (X_OS and X_OS_TE) in this dataset. When compared to each other, X_TE is superior to RF + ET. This motivates the usage of tree-embeddings in other applications with larger label sets. Furthermore, at this point, it can be deduced that methods which use directly the output variables to augment the input feature space, such as MLDF, could not be applied to extreme multi-label data. They would lead to extremely high dimensional feature sets, dramatically increasing their computational demands.

In some datasets, such as scene and yeast, the performance from most of evaluated methods was close to flawless. Differently from that, unexpected results were obtained in the CAL500 dataset considering the one error measure. This could be explained by its substantial number of possible labels (174) and its relatively low label cardinality (26.04) which can often lead to wrong predictions being ranked as first.

6. Conclusion

In this paper, we have proposed a novel deep tree-ensemble model for multi-output prediction tasks which can integrate tree-embeddings as well as output features in the learning process. Our results have shown that our model provides superior results in both multi-target regression and multi-label classification.

More precisely, they reveal that integrating a representation learning component in each layer can significantly boost prediction performance, affirming our original hypothesis. Tree-embeddings can be more meaningful than just output features in both tasks. Additionally, in some cases, the combination of both can boost the performance even further. We also highlight that preserving the original feature set is essential to achieve high performance, since the tree-embeddings variant rarely yields superior results by itself.

As for future work, we would like to exploit different ensembles of trees. That is, explore if the inclusion of other tree-based ensembles can improve the results, such as predictive bi-clustering trees [38] [39], extreme gradient boosting [40] and oblique forests [41].

Furthermore, other multi-output tasks such as hierarchical multi-label classification [42] and extreme multi-label classification [43] may also be addressed with our method, specially because the MLDF would result in a very high number of features whereas the tree-embeddings would be unaffected.

Acknowledgements

The authors acknowledge the support from the Research Fund Flanders (through research project G080118N) and from the Flemish Government (AI Research Program).

References

- [1] S. Yin, X. Li, H. Gao, O. Kaynak, Data-based techniques focused on modern industry: An overview, *IEEE Transactions on Industrial Electronics* 62 (1) (2015) 657–667.

- [2] M. I. Jordan, T. M. Mitchell, Machine learning: Trends, perspectives, and prospects., *Science* 349 (6245) (2015) 255–260.
- [3] A. Esteva, B. Kuprel, R. A. Novoa, J. Ko, S. M. Swetter, H. M. Blau, S. Thrun, Dermatologist-level classification of skin cancer with deep neural networks, *nature* 542 (7639) (2017) 115–118.
- [4] G. Eraslan, Ž. Avsec, J. Gagneur, F. J. Theis, Deep learning: new computational modelling techniques for genomics, *Nature Reviews Genetics* 20 (7) (2019) 389–403.
- [5] C. Badue, R. Guidolini, R. V. Carneiro, P. Azevedo, V. B. Cardoso, A. Forechi, L. Jesus, R. Berriel, T. M. Paixão, F. Mutz, L. de Paula Veronese, T. Oliveira-Santos, A. F. De Souza, Self-driving cars: A survey, *Expert Systems with Applications* 165 (2021) 113816. doi:<https://doi.org/10.1016/j.eswa.2020.113816>.
URL <http://www.sciencedirect.com/science/article/pii/S095741742030628X>
- [6] I. H. Witten, E. Frank, M. A. Hall, *Data Mining: Practical Machine Learning Tools and Techniques*, 4th Edition, Morgan Kaufmann, 2016. arXiv:arXiv:1011.1669v3.
- [7] W. Waegeman, K. Dembczyński, E. Hüllermeier, Multi-target prediction: a unifying view on problems and methods, *Data Mining and Knowledge Discovery* 33 (2) (2019) 293–324.
- [8] G. Tsoumakas, I. Katakis, I. Vlahavas, *Mining Multi-label Data*, Springer US, Boston, MA, 2010, pp. 667–685. doi:10.1007/978-0-387-09823-4_34.
URL https://doi.org/10.1007/978-0-387-09823-4_34
- [9] Z.-H. Zhou, J. Feng, Deep forest: Towards an alternative to deep neural networks, in: *Proceedings of the Twenty-Sixth International Joint Conference on Artificial Intelligence, IJCAI-17, 2017*, pp. 3553–3559. doi:

10.24963/ijcai.2017/497.

URL <https://doi.org/10.24963/ijcai.2017/497>

- [10] L. Breiman, Random forests, *Machine learning* 45 (1) (2001) 5–32.
- [11] C. Vens, F. Costa, Random forest based feature induction, in: 2011 IEEE 11th International Conference on Data Mining, IEEE, 2011, pp. 744–753.
- [12] K. Pliakos, C. Vens, Mining features for biomedical data using clustering tree ensembles, *Journal of biomedical informatics* 85 (2018) 40–48.
- [13] D. Xu, Y. Shi, I. W. Tsang, Y.-S. Ong, C. Gong, X. Shen, Survey on multi-output learning, *IEEE transactions on neural networks and learning systems*.
- [14] H. Borchani, G. Varando, C. Bielza, P. Larrañaga, A survey on multi-output regression, *Wiley Interdisciplinary Reviews: Data Mining and Knowledge Discovery* 5 (5) (2015) 216–233.
- [15] H. Blockeel, L. De Raedt, Top-down induction of first-order logical decision trees, *Artificial intelligence* 101 (1-2) (1998) 285–297.
- [16] S. M. Mastelini, E. J. Santana, R. Cerri, S. Barbon, Dstars: A multi-target deep structure for tracking asynchronous regressor stacking, *Applied Soft Computing* 91 (2020) 106215. doi:<https://doi.org/10.1016/j.asoc.2020.106215>.
URL <http://www.sciencedirect.com/science/article/pii/S1568494620301551>
- [17] G. Tsoumakas, I. Vlahavas, Random k-labelsets: An ensemble method for multilabel classification, in: J. N. Kok, J. Koronacki, R. L. d. Mantaras, S. Matwin, D. Mladenič, A. Skowron (Eds.), *Machine Learning: ECML 2007*, Springer Berlin Heidelberg, Berlin, Heidelberg, 2007, pp. 406–417.
- [18] D. Kocev, M. Ceci, T. Stepišnik, Ensembles of extremely randomized predictive clustering trees for predicting structured outputs, *Machine Learning* (2020) 1–29.

- [19] D. Kocev, C. Vens, J. Struyf, S. Džeroski, Tree ensembles for predicting structured outputs, *Pattern Recognition* 46 (3) (2013) 817–833.
- [20] J. Du, Y. Xu, Hierarchical deep neural network for multivariate regression, *Pattern Recognition* 63 (2017) 149–157.
- [21] X. Zhen, M. Yu, Z. Xiao, L. Zhang, L. Shao, Heterogenous output regression network for direct face alignment, *Pattern Recognition* (2020) 107311.
- [22] E. Spyromitros-Xioufis, G. Tsoumakas, W. Groves, I. Vlahavas, Multi-target regression via input space expansion: treating targets as inputs, *Machine Learning* 104 (1) (2016) 55–98.
- [23] M.-L. Zhang, Z.-H. Zhou, Ml-knn: A lazy learning approach to multi-label learning, *Pattern Recognition* 40 (7) (2007) 2038 – 2048.
doi:<https://doi.org/10.1016/j.patcog.2006.12.019>.
URL <http://www.sciencedirect.com/science/article/pii/S0031320307000027>
- [24] R. Wang, S. Kwong, X. Wang, Y. Jia, Active k-labelsets ensemble for multi-label classification, *Pattern Recognition* 109 107583.
- [25] Z. Ma, S. Chen, Expand globally, shrink locally: Discriminant multi-label learning with missing labels, *Pattern Recognition* (2020) 107675.
- [26] L. Yang, X.-Z. Wu, Y. Jiang, Z.-H. Zhou, Multi-label learning with deep forest, arXiv preprint arXiv:1911.06557.
- [27] P. Geurts, D. Ernst, L. Wehenkel, Extremely randomized trees, *Machine learning* 63 (1) (2006) 3–42.
- [28] Q.-W. Wang, L. Yang, Y.-F. Li, Learning from weak-label data: A deep forest expedition., in: *AAAI, 2020*, pp. 6251–6258.
- [29] J. Gao, K. Liu, B. Wang, D. Wang, Q. Hong, An improved deep forest for alleviating the data imbalance problem, *Soft Computing* (2020) 1–17.

- [30] N. V. Chawla, K. W. Bowyer, L. O. Hall, W. P. Kegelmeyer, Smote: synthetic minority over-sampling technique, *Journal of artificial intelligence research* 16 (2002) 321–357.
- [31] R. Su, X. Liu, L. Wei, Q. Zou, Deep-resp-forest: A deep forest model to predict anti-cancer drug response, *Methods* 166 (2019) 91–102.
- [32] C. Ma, Z. Liu, Z. Cao, W. Song, J. Zhang, W. Zeng, Cost-sensitive deep forest for price prediction, *Pattern Recognition* 107 (2020) 107499.
- [33] M. Zhou, X. Zeng, A. Chen, Deep forest hashing for image retrieval, *Pattern Recognition* 95 (2019) 114–127.
- [34] O. Sagi, L. Rokach, Ensemble learning: A survey, *Wiley Interdisciplinary Reviews: Data Mining and Knowledge Discovery* 8 (4) (2018) e1249.
- [35] J. Read, B. Pfahringer, G. Holmes, E. Frank, Classifier chains for multi-label classification, in: *Joint European Conference on Machine Learning and Knowledge Discovery in Databases*, Springer, 2009, pp. 254–269.
- [36] D. H. Wolpert, Stacked generalization, *Neural networks* 5 (2) (1992) 241–259.
- [37] J. Read, B. Pfahringer, G. Holmes, E. Frank, Classifier chains: A review and perspectives, *arXiv preprint arXiv:1912.13405*.
- [38] K. Pliakos, C. Vens, Network inference with ensembles of bi-clustering trees, *BMC bioinformatics* 20 (1) (2019) 525.
- [39] B. Zamith, F. K. Nakano, R. Cerri, C. Vens, Predictive bi-clustering trees for hierarchical multi-label classification, *ECML PKDD 2020*.
- [40] T. Chen, C. Guestrin, Xgboost: A scalable tree boosting system, in: *Proceedings of the 22nd acm sigkdd international conference on knowledge discovery and data mining*, 2016, pp. 785–794.

- [41] R. Katuwal, P. N. Suganthan, L. Zhang, Heterogeneous oblique random forest, *Pattern Recognition* 99 (2020) 107078.
- [42] F. K. Nakano, M. Lietaert, C. Vens, Machine learning for discovering missing or wrong protein function annotations, *BMC bioinformatics* 20 (1) (2019) 485.
- [43] K. Bhatia, H. Jain, P. Kar, M. Varma, P. Jain, Sparse local embeddings for extreme multi-label classification, in: *Advances in neural information processing systems*, 2015, pp. 730–738.